



ACTIVE VIBRATION CONTROL OF A LAMINATED COMPOSITE BEAM USING *MFRC* PATCHES

Ping Tan*, Liyong Tong **

* School of Aerospace, Mechanical and Mechatronic Engineering
University of Sydney, NSW 2006, Australia,

** School of Aerospace, Mechanical and Mechatronic Engineering
University of Sydney, NSW 2006, Australia

Keywords: active vibration control, dynamic analytical model, *MFRC* sensor and actuator

Abstract

This paper focuses on modeling development for active vibration control of a laminated beam, which is bonded with magnetostrictive fiber reinforced composite (*MFRC*) and excited by an impulsive force. Two dynamic analytical models are developed using the Euler-Bernoulli theory and Timoshenko's theory of beams, respectively. A feedback control algorithm coupling the *MFRC* sensor and actuator is used. The active control magnetic field is applied to the *MFRC* actuator encircled by an actuation coil, and the required magnetic flux density is obtained from the sensing coil encircling the *MFRC* sensor. It is revealed from the numerical study that for the considered cases, the *MFRC* patches is more effective for vibration suppression of a beam than the piezoelectric fiber reinforced composite (*PFRC*) patches. A comparison of the natural frequencies for the beams with various *MFRC* patches is conducted between the present analytical and finite element analysis models. A good agreement is noted.

1 Introduction

Flexible structural members, such as beams, have been widely used in industry, and vibration control and performance improvement of such structures are important issues in practice, e.g., precise operation and control of aerospace systems, satellites, etc. However, due to the complexity of dynamics of flexible structures, vibration control using various active materials, such as piezoelectric and its composite materials [1-4], has drawn a significant attention of researchers over the past decades. This is owing to that the coupled electromechanical properties of piezoelectric ceramics and their availability in the form of thin

sheets make them well suited for use as sensors and actuators for controlling structural response [2]. Similarly, magnetostriction is the phenomenon of strong coupling between magnetic and mechanical properties of some ferromagnetic materials, in which strains are generated in response to an applied magnetic field, while conversely, mechanical stresses in the materials produce measurable changes in magnetization. This phenomenon can be used for actuation and sensing [5].

Recently, magnetostrictive materials are being increasingly used as both sensors and actuators for active vibration control due to their advantages such as the possibility of remote excitation and easy embedability into the host material and structure. In particular, the magnetostrictive particles can be embedded into laminated composite structures without compromising the structural integrity. For example, Murty et al [6] investigated the feasibility of using an embedded Terfenol-D particle layer for the vibration suppression capability of a flexible cantilever laminated composite beam. Kumar et al derived a finite element formulation for the damping characteristics of an aluminum beam bonded with a distributed magnetostrictive layer under different boundary conditions and coil configurations [7], followed by analyzing the damping characteristics of a titanium shell with a magnetostrictive layer [8]. Lee et al [9] applied a unified plate theory, including the classical, first-order, and third-order plate theories, to study the control of the transient response of laminated composite plates with Terfenol-D magnetostrictive layers, used as sensors and actuators. Pradhan [10] used the first-order shear deformation theory to study vibration control of functionally graded shells with embedded magnetostrictive layers. However, the application of magnetostrictive materials has been limited in

practice due to the factors such as brittleness in tension and development of eddy currents that limit the frequency range. At present, magnetostrictive composites, which are manufactured by combining a particle or fibre form of magnetostrictive material with polymer binder, attract much attention due to their advantages over the monolithic magnetostrictive materials such as less brittleness and large operation frequency bandwidth. This will lead to the application of these composites in active vibration control.

In this paper, two dynamic analytical models are proposed for active vibration suppression of a laminated beam bonded with collocated or non-collocated magnetostrictive fiber reinforced composite (*MFRC*) patches. These two models are developed using the Euler-Bernoulli theory and Timoshenko's theory of beams, respectively, under the assumption of constant peel and shear strains through the bond line thickness [11]. A feedback control algorithm coupling the *MFRC* sensor and actuator is used. The active control electric field is applied to the actuation coil encircling the *MFRC* actuator, and the required magnetic flux density is obtained from the sensing coil which encircles the *MFRC* sensor.

A numerical study is carried for discussing the effects of the major parameters of the *MFRC* patches such as the location of *MFRC* sensor, fiber volume fraction V_f and orientation angle θ of *MFRC* patch on the amplitude change of the free end deflection (*ACFED*) for a cantilever laminated beam. Subsequently, a comparison of the *ACFED* for the beam bonded with collocated *MFRC* sensor and actuator pair is conducted between the model developed using the Euler-Bernoulli theory and that using Timoshenko's theory of beams. Also, the values of *ACFED* for the Timoshenko's beam bonded with collocated *MFRC* sensor and actuator pair are compared with those bonded with collocated *PFRC* sensor and actuator pair. For verifying the present analytical models, the first three frequencies for the beam systems bonded with collocated *MFRC* patches and having various values of V_f and θ are compared between the present analytical and finite element analysis (*FEA*) models, and a good agreement is noted.

2 Dynamic Analytical Models for Vibration Control

Two laminated carbon fiber reinforced composite beam systems surface bonded with collocated or non-collocated *MFRC* actuator and sensor pair are considered in this study (see Fig. 1 for the case of collocated *MFRC* sensor and actuator pair and Fig. 2 for the non-collocated *MFRC* sensor and actuator pair). The *MFRC* actuator encircled by an actuation coil is used to generate the actuation stress on the top surface of the beam for the suppression of structural vibration, and the *MFRC* sensor encircled by a sensing coil is employed to measure the magnetic flux density passing through the *MFRC* sensor, which is closely related to the strain along the beam segment bonded with a *MFRC* sensor. A feedback control model using a magnetic flux density control amplifier of gain K_B is used for active vibration control of the laminated beam. The magnetic field applied to the *MFRC* actuator is directly proportional to magnetic flux density through the sensing coil.

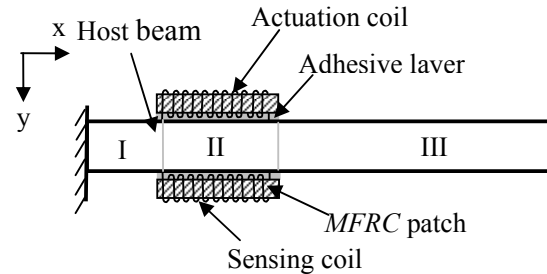


Fig.1. A cantilever laminated beam bonded with collocated *MFRC* actuator and sensor patches

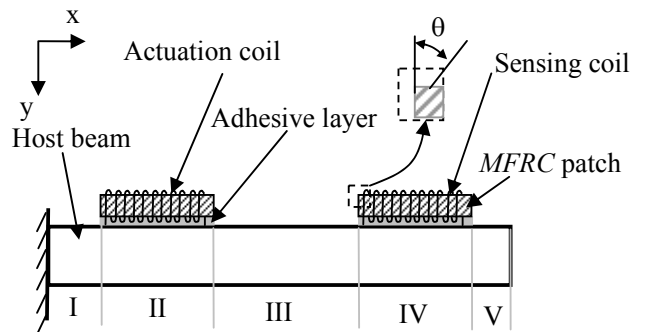


Fig.2. A cantilever laminated beam bonded with non-collocated *MFRC* actuator and sensor patches

For active vibration control of a laminated beam using MFRC actuator and sensor pair, two dynamic analytical models are presented. One is developed using the Euler-Bernoulli theory and the other is established using Timoshenko's theory of beams under the assumptions of constant peel and shear strains through the bond line thickness [11]. In this study, the MFRC patches are assumed to be perfectly bonded on the beam surfaces. Since the governing equations are different for the beam segments bonded with and without MFRC actuator or sensor, we divide the beam system into three pan-wise regions for the case shown in Fig. 1 and five regions for the case shown in Fig.2. The MFRC and beam segments in each region are considered as an Euler-Bernoulli beam or Timoshenko's beam. Based on the corresponding beam theory and the assumptions mentioned previously, the required dynamic equations of motion for each component segment can be derived. For example, the dynamic equations of motion for the MFRC actuator and beam segments located in region II in Fig. 2 are given as follows

(1) For the MFRC actuator:

$$\rho_a A_a \ddot{u}_{2a} = \frac{\partial T_{2a}}{\partial x} + \tau_2 W \quad (1)$$

$$\rho_a A_a \ddot{w}_{2a} = \frac{\partial Q_{2a}}{\partial x} + \sigma_2 W \quad (2)$$

$$\frac{\partial M_{2a}}{\partial x} - Q_{2a} + \frac{\tau_2 t_a W}{2} = 0 \quad (3)$$

(2) For the laminated beam segment

$$\rho_b A_b \ddot{u}_{2b} = \frac{\partial T_{2b}}{\partial x} - \tau_2 W \quad (4)$$

$$\rho_b A_b \ddot{w}_{2b} = \frac{\partial Q_{2b}}{\partial x} - \sigma_2 W \quad (5)$$

$$\frac{\partial M_{2b}}{\partial x} - Q_{2b} + \frac{\tau_2 W t_b}{2} = 0 \quad (6)$$

where $T_{2a} = WY_a t_a \frac{\partial u_{2a}}{\partial x} - q_{11a} W t_a H_1$,

$T_{2b} = WY_b t_b \frac{\partial u_{2b}}{\partial x}$, $M_{2i} = -\frac{WY_i t_i^3}{12} \frac{\partial^2 w_{2i}}{\partial x^2}$ for the

case using Euler-Bernoulli theory and

$M_{2i} = -\frac{WY_i t_i^3}{12} \frac{\partial \psi_{2i}}{\partial x}$ for the case using

Timoshenko's theory of beams ($i=a$ for actuator and b for the host beam), $a, b, \rho, A, Y, W, t, q_{11}, Q, T, M, \tau, \sigma, H_1, \mu, w$ and ψ stand for the MFRC actuator, laminated beam, density, cross-sectional area, complex Young's modulus, width of beam system, thickness, piezomagnetic constant for the MFRC patch subjected to an electric field in the I or x direction, shear force, longitudinal force, bending moment, shear and peel stresses in the adhesive layer between the MFRC actuator and host laminated beam, magnetic field applied to the MFRC actuator segment along the x or I direction, longitudinal displacement, transverse displacement and the deflection angle of the cross-section of the beam with respect to the vertical direction, respectively. For the shear and peel stresses under the assumptions of constant peel and shear strains through the adhesive layer thickness in adhesively bonded joints [11], they can be evaluated using the Eqs. (3-5) in Ref.[12] for the case using Euler-Bernoulli theory and Eqs. (7-8) below for the case using Timoshenko's theory of beams.

$$\tau_{2a} = G_{ad} \left\{ \frac{1}{2} (\psi_{2a} + \psi_{2b}) + \frac{1}{2t_{ad}} (t_a \psi_{2a} + t_b \psi_{2b}) + \frac{u_{2b} - u_{2a}}{t_{ad}} \right\} \quad (7)$$

$$\sigma_{2a} = \frac{Y_{ad}(1-\nu_{ad})}{(1-2\nu_{ad})(1+\nu_{ad})t_{ad}} (w_{2b} - w_{2a}) \quad (8)$$

where G and ν are the shear modulus and Poisson's ratio whereas the subscript ab stands for the adhesive layer.

For the beam system shown in Fig. 1, a total of 12 continuity conditions exist at the interface between region I and II as well as II and III, whereas for that shown in Fig. 2, a total of 24 continuity conditions exist at the interface between region I and II to IV and V. They are given as follows

$$u_{ib} = u_{(i+1)b}, \quad w_{ib} = w_{(i+1)b}, \quad T_{ib} = T_{(i+1)b},$$

$$Q_{ib} = Q_{(i+1)b}, \quad M_{ib} = M_{(i+1)b},$$

$\frac{\partial w_{ib}}{\partial x} = \frac{\partial w_{(i+1)b}}{\partial x}$ (for the case using Euler-Bernoulli beam) or $\psi_{ib} = \psi_{(i+1)b}$ (for the case using Timoshenko's beam).

For the beam system bonded with collocated or non- collocated *MFRC* actuator and sensor pair, a total of 18 boundary conditions can be obtained and are listed as below

(1) For the actuator

$$T_{la} = 0, Q_{la} = 0, M_{la} = 0, T_{ra} = 0, Q_{ra} = 0, M_{ra} = 0.$$

(2) For the sensor

$$T_{ls} = 0, Q_{ls} = 0, M_{ls} = 0, T_{rs} = 0, Q_{rs} = 0, M_{rs} = 0.$$

(3) For the host beam

$$u_{lb} = 0, w_{lb} = 0, \frac{\partial w_{lb}}{\partial x} = 0 \text{ (for the case using Euler-Bernoulli beam) or } \psi_{lb} = 0 \text{ (for the case using Timoshenko's beam), } T_{rb} = 0, Q_{rb} = 0, M_{rb} = 0.$$

where l stands for left hand side of the segment and r stands for the right hand side of the segment.

By numerically solving the dynamic equations of motion for all component segments together with their boundary and continuity conditions, the required natural frequencies (ω_i) and average value of the strain (ε_{savg}) induced in the *MFRC* sensor which is encircled by the sensing coil can be obtained. Thus, for a selected natural frequency ω , the magnetic flux density $B_s(X_s, \omega)$ passing through the sensing coil with zero applied magnetic field H_1 and located at a distance of X_s from the fixed end of the beam can be obtained by

$$B_s(X_s, \omega) = q_{11} |\varepsilon_{savg}(X_s, \omega)| \quad (9)$$

Considering the magnetic flux density feedback control with the control gain K_B , the magnetic field H_1 can be obtained by

$$H_1(X_a, \omega) = K_B B_s(X_s, \omega) \quad (10)$$

where X_a is the distance of the *MFRC* actuator centre from the fixed end of the beam.

3 Parametric Study

In order to study the performance of *MFRC* actuator and sensor for active vibration control of a laminated composite beam, a baseline case with the beam length of 0.3m, width of 0.02m and thickness of 1.9mm is considered. The thickness of the *MFRC* patch and adhesive layer are chosen to be 0.4mm and 0.15mm. The width and length of the *MFRC* sensor and actuator are selected to be 0.02m and 0.06m, respectively. The value of X_a is chosen to be 0.09m whereas the value of X_s is selected to be 0.09m for the case of collocated *MFRC* actuator and sensor pair and 0.21m for the case of non-collocated *MFRC* pair. The required complex Young's modulus for the host beam made of *T300/GY260* plain weave composite and adhesive layer are chosen as 65.68(1+0.011i)GPa, and 2.15(1+0.011i)GPa, respectively [13]. The density for the host beam, magnetostrictive material *CoFe₂O₄*, matrix and adhesive layers are selected to be 1527.38kg/m³, 5300kg/m³, 1200kg/m³ and 1600 kg/m³, respectively. For *MFRC* patches with different fiber volume fraction V_f and orientation angle θ , their corresponding Young's modulus and piezomagnetic coefficients can be evaluated using the analytical model previously developed by the authors for the piezoelectric/magnetostrictive composite behavior [14] and the corresponding transformation matrix. The properties for the magnetostrictive material *CoFe₂C₄* and matrix are listed in Tables 1 and 2 [15-16]. In this study, the control gain K_B is selected to be 3×10^5 Am/Wb. By using the analytical model developed using the Euler-Bernoulli theory and the corresponding data for the baseline case, the variation trend of *ACFED* for the beam system shown in Figs. 1-2 with V_f and θ can be obtained, and plotted in Figs.3 for the case of $\theta=60^\circ$ and Fig. 4 for the case of $V_f=0.6$, where the *ACFED* is obtained using the following Eq.(11), in which *FED* stands for free end deflection of the laminated beam.

$$ACFED = \frac{FED_{before\ using\ control\ law} - FED_{after\ using\ control\ law}}{FED_{before\ using\ control\ law}} \times 100\% \quad (11)$$

Table 1. Properties for CoFe₂C₄ [15]

C ₁₁ =C ₂₂ (GPa)	C ₁₂ (GPa)	C ₁₃ =C ₂₃ (GPa)	C ₃₃ (GPa)
286	173	170	269.5
C ₄₄ =C ₅₅ (GPa)	C ₆₆ (GPa)	q ₃₁ =q ₃₂ (m/A)	q ₃₃ (m/A)
45.3	56.5	580.3	699.7
q ₁₅ =q ₂₄ (m/A)	μ ₁₁ (10 ⁻⁶ NS ² /C ²)	μ ₂₂ (10 ⁻⁶ NS ² /C ²)	μ ₃₃ (10 ⁻⁶ NS ² /C ²)
550	-590	-590	157

Table 2. Properties for matrix [16]

C ₁₁ =C ₂₂ (GPa)	C ₁₂ (GPa)	C ₁₃ =C ₂₃ (GPa)	C ₃₃ (GPa)	C ₄₄ =C ₅₅ =C ₆₆ (GPa)
3.74	1.12	1.12	3.74	1.31

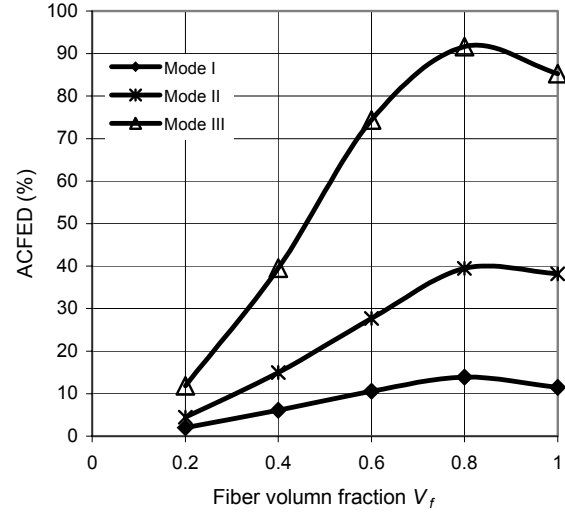
Table 3. Properties for PZT [17]

C ₁₁ =C ₂₂ (GPa)	C ₁₂ (GPa)	C ₁₃ =C ₂₃ (GPa)	C ₃₃ (GPa)	C ₄₄ =C ₅₅ =C ₆₆ (GPa)
84.81	36.35	36.35	84.81	24.0
e ₃₁ =e ₃₂ (C/m ²)	e ₃₃ (C/m ²)	e ₁₅ =e ₂₄ (C/m ²)	ε ₃₁ =ε ₃₂ (10 ⁻⁹ F/m)	ε ₃₃ (10 ⁻⁹ F/m)
44.37	50.18	14.02	7.11	-26.0

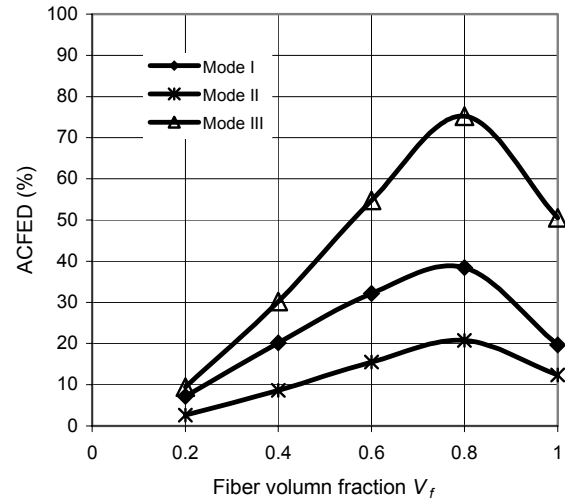
From Figs. 3-4, we noted that for the beam system with the collocated or non-collocated MFRC actuator and sensor pair, the values of *ACFED* increases significantly with V_f and θ until $V_f=0.8$ and $\theta=60^\circ$, beyond those, the *ACFED* changes slightly except for the case shown in Fig. 3(b), in which *ACFEDs* for the case of mode *I* and *III* decrease significantly with V_f when V_f attains to 0.8. This may be caused by that the Young's modulus of the MFRC patch increases significantly when V_f and θ attains to 0.8 and 60° , respectively (see Fig. 5(a) and 6(a) in Ref. [13]). From Figs. 3-4, it is interesting to note that for the case of mode *I*, the values of *ACFED* for the collocated MFRC pair are greater than those for the non-collocated MFRC pair, whereas for the case of mode *II* and *III*, the values of *ACFED* for the collocated MFRC pair are less than those for the non-collocated MFRC pair.

Figure 5 shows the variation trends of *ACFED* with V_f and θ for a beam system bonded with collocated MFRC pair, which are obtained using the analytical model developed based on the Timoshenko's theory of beams. A comparison between Fig. 3(b) and Fig. 5(a) and that between Fig. 4(b) and Fig. 5(b) indicate that there is a good

agreement between the *ACFED* values predicted using the Euler-Bernoulli theory and Timoshenko's theory of beams. The differences of between them range from 0.36-6.9 % for the case of mode *I*, 0-4.8% for the mode *II* and 0.2-6.9% for the mode *III*.

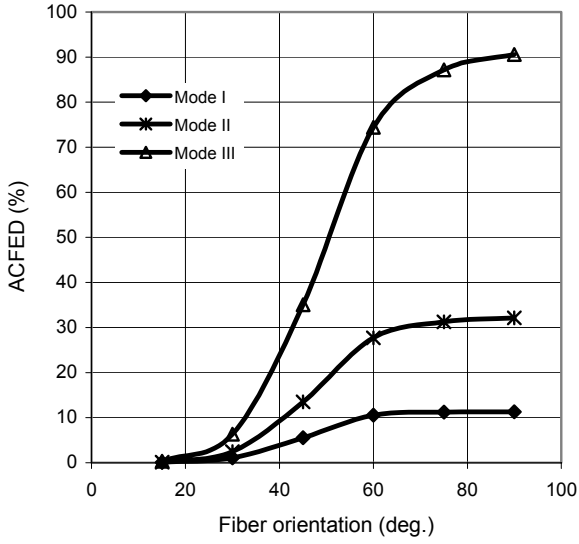


(a) For the non-collocated MFRC pair

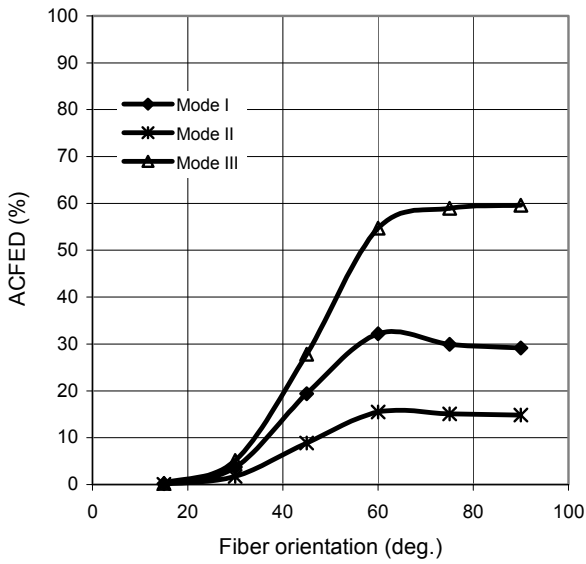


(b) For the collocated MFRC pair

Fig. 3. Variation trends of *ACFED* with fiber volume fraction V_f for the cases of vibration mode *I* to *III* and $\theta=60^\circ$.

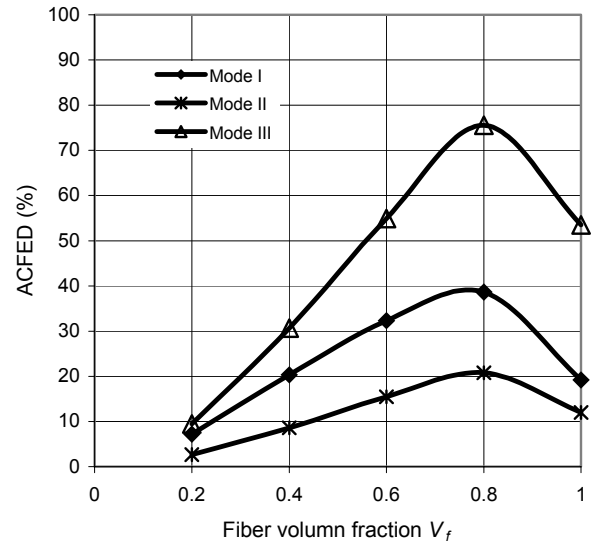


(a) For the non-collocated *MFRC* pair

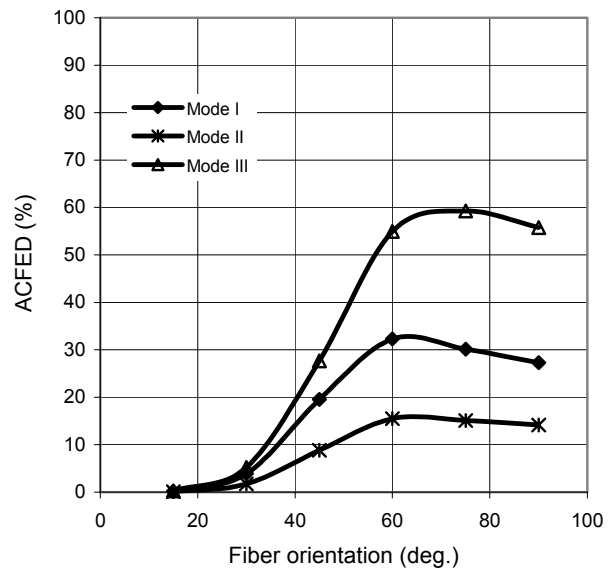


(b) For the collocated *MFRC* pair

Fig. 4. Variation trends of *ACFED* with fiber orientation θ for the cases of vibration mode *I* to *III* and $V_f=0.6$.



(a) For the case of $\theta=60^\circ$



(b) For the case of $V_f=0.6$

Fig. 5. Variation trends of *ACFED* with V_f and θ for the cases of vibration mode *I* to *III* and having collocated *MFRC* pair .

For the sake of comparing the vibration suppression capability of a laminated beam bonded with the collocated MFRC actuator and sensor pair with that having the collocated PFRC actuator and sensor pair, the dynamic analytical model using the Timoshenko's theory of beams and collocated MFRC actuator and sensor pair is modified by replacing the MFRC pair with the PFRC pair to evaluate the ACFED values for the beam bonded with the PFRC patches. By using the analytical model for the PFRC pair and the required data, which are the same as the those for the baseline case previously mentioned for the MFRC patch, except for that the properties of the MFRC patch are replaced by those for the PFRC patch, the ACFED values for the beam bonded with PFRC patches can be obtained. The Young's modulus and piezoelectric coefficients for the PFRC patches with various values of V_f and θ can be obtained by following the similar procedure for predicting the properties of MFRC patches mentioned previously. The electromechanical properties for the piezoelectric material PZT are listed in Table 3 [17]. The density for the PZT is selected to be 7600kg/m^3 . An electric displacement (or electric flux density) feedback control algorithm with the control gain K_B is employed here, and thus the electric field E_f applied to the PFRC actuator along the x direction can be obtained by

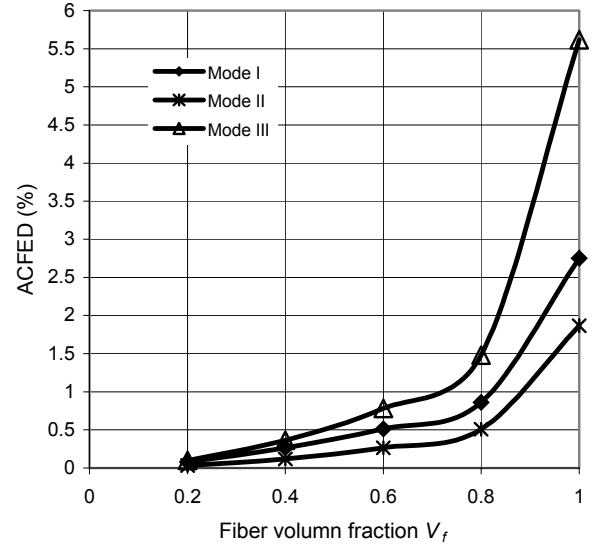
$$E_1(X_a, \omega) = K_B D_s(X_s, \omega) \quad (12)$$

where electric displacement is evaluated by

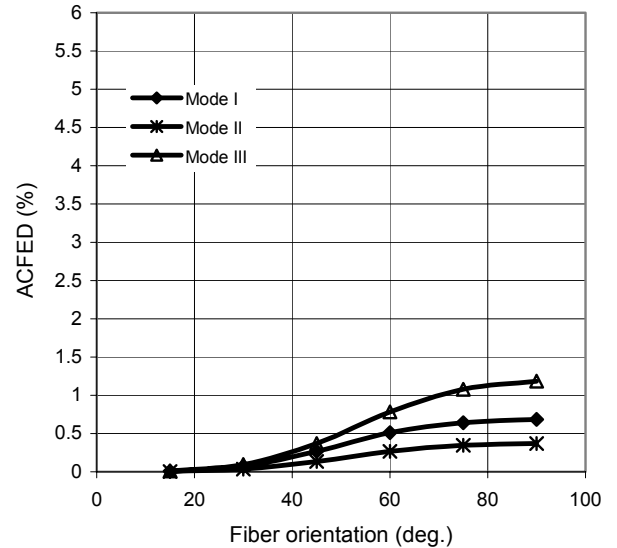
$$D_s(X_s, \omega) = e_{11} \left| \varepsilon_{savg}(X_s, \omega) \right| \quad (13)$$

Figure 6 illustrates the variation trends of ACFED with V_f and θ for the cases of a laminated beam bonded with collocated PFRC pair. A comparison of Fig. 5 and Fig. 6 reveals that the variation patterns of ACFED with V_f for the case with MFRC pair are different from those with PFRC pair, whereas the variation trends of ACFED with θ between them are similar until $\theta = 60^\circ$, beyond that the ACFED values slightly decrease with θ for the case with MFRC pair but slightly increase with θ for the case with PFRC pair. In addition, it is noted by comparing Fig. 5 with Fig.6 that the ACFED values for the case using collocated MFRC pair are much larger than those using collocated PFRC pair.

Thus, for the cases considered here, it is preferred to choose the MFRC pair for active vibration control of a laminated composite beam due to their high ACFED value and low density.



(a) For the case of $\theta=60^\circ$



(b) For the case of $V_f=0.6$

Fig. 6. Variation trends of ACFED with V_f and θ for the cases of collocated PFRC pair and vibration mode I to III.

4 Verification

To verify the present analytical model, several 2D plane strain *FEA* models for a cantilever laminated beam bonded with various *MFRC* actuator and sensor pair are established using the *FEA* software Strand7 [18]. For the beam systems bonded with the collocated *MFRC* patches having various values of V_f and θ , their corresponding first three frequencies, which are predicted using the present *FEA* and analytical models, are tabulated in Tables 4-5, where Analy_E stands for the analytical model developed using the Euler-Bernoulli theory whereas Analy_T refers to the analytical model established using the Timoshenko's theory of beams.

Table 4. Comparisons of the natural frequencies with fiber volume fraction V_f predicted by the *FEA*, analytical models for the beam system bonded with collocated *MFRC* pair

V_f	Mode I (Hz)		
	FEA	Analy-E	Analy-T
0.2	23.482	23.24	23.25
0.4	23.88	23.62	23.63
0.6	24.2	23.95	23.97
0.8	24.56	24.32	24.34
1	25.27	25.27	25.3
V_f	Mode II (Hz)		
	FEA	Analy-E	Analy-T
0.2	133.49	134.66	134.9
0.4	132.16	133.06	133.3
0.6	130.9	131.61	131.87
0.8	129.99	130.58	130.84
1	130.77	132.01	132.38
V_f	Mode III (Hz)		
	FEA	Analy-E	Analy-T
0.2	376.17	378.01	379.68
0.4	378.2	378.03	379.72
0.6	380.88	379.18	380.99
0.8	386.55	383.85	396.68
1	409.71	414.66	401.24

Table 5. Comparisons of the natural frequencies with fiber orientation θ predicted by the *FEA*, analytical models for the beam system bonded with collocated *MFRC* pair

θ	Mode I (Hz)		
	FEA	Analy-E	Analy-T
15°	23.21	23	23.01
30°	23.27	23.04	23.05
45°	23.56	23.31	23.32
60°	24.2	23.95	23.97
75°	24.72	24.48	24.50
90°	24.84	24.62	24.64
θ	Mode II (Hz)		
	FEA	Analy-E	Analy-T
15°	127.7	128.74	128.98
30°	127.94	128.88	129.12
45°	128.83	129.67	129.91
60°	130.9	131.61	131.87
75°	132.53	133.24	133.52
90°	132.95	133.67	133.96
θ	Mode III (Hz)		
	FEA	Analy-E	Analy-T
15°	356.27	356.94	358.4
30°	357.38	357.89	359.36
45°	363.84	363.56	365.11
60°	380.88	379.18	380.99
75°	396.54	394.48	396.68
90°	400.88	398.91	401.24

From Tables 4-5, it is noted that there is a good agreement between the present analytical and *FEA* models. The difference between the *FEA* and analytical model with Euler-Bernoulli beam ranges 0-1.1 % for the case of mode I, 0.45-0.81% for the mode II, 0.04-1.21% for the mode III, whereas the difference between the *FEA* and analytical model using Timoshenko beam ranges 0.08-1.05% for the mode I, 0.6-1.2% for the mode II, 0.03-2.62 % for the mode III. In addition, Tables 4-5 reveal that the variation trends of the natural frequencies with V_f and θ , which are obtained using the *FEA* and analytical models, are consistent well.

5 Conclusions

In this paper, two dynamic analytical models are developed using the Euler-Bernoulli theory and Timoshenko's theory of beams, followed by using these two models for active vibration suppression of a cantilever laminated beam bonded with MFRC actuator and sensor pair. For the case considered here, it is revealed from the numerical study that the collocated MFRC pair is more effective for active vibration suppression of a flexible beam than the non-collocated MFRC pair for the case of mode I, whereas for the case of mode II and III, vibration suppression capability of the beam with non-collocated MFRC pair is better than that with collocated MFRC pair. It is also noted that for both cases of collocated and non-collocated MFRC actuator and sensor pair, the values of ACFED are closely related to V_f and θ . In general, they increase significantly with V_f and θ until $V_f=0.8$ and $\theta=60^\circ$, beyond those, the ACFED changes slightly. A comparison of the variation trends of ACFED with V_f and θ obtained using the present analytical models with the Euler-Bernoulli beam and Timoshenko beam shows that there is a good agreement between them. It is also noted from the numerical study that the ACFED values for the case with collocated MFRC pair are much larger than those with collocated PFRC pair, and thus for the cases considered here, it is recommended to choose the MFRC pair for active vibration control of a laminated composite beam. Finally, the proposed analytical models are verified by showing a good agreement between the natural frequencies predicted using the present FEA and analytical models.

Acknowledgement

The authors are grateful to the support of University of Sydney via University Postdoctoral Research Fellowship.

References

- [1] Hu Y.R. and Ng A. "Active robust vibration control of flexible structures". *Journal of Sound and Vibration*, Vol. 288, No. 1-2, pp 43-56, 2001.
- [2] Narayanan S and Balamurugan V. "Finite element modelling of piezolaminated smart structures for active vibration control with distributed sensors and actuators". *Journal of Sound and Vibration*, Vol.262, No.3, pp 529-562, 2003.
- [3] Tan P and Tong L. "Active vibration control of a beam system with APFRC damping layers," *Proceedings of the 10th US-Japan Conference on Composite materials*, Stanford University, USA, pp 190-198, 2002.
- [4] Tan P, Tong L and Sun D.C. "Dynamic characteristics of a beam system with active piezoelectric fiber reinforced composite layers," *Composites, Part B: Engineering*, Vol. 33, No. 7, pp 545-555, 2002.
- [5] Tan X B and Baras J S. "Modeling and control of hysteresis in magnetostrictive actuators". *Automatica*, Vol. 40, No. 9, pp 1469-1480, 2004.
- [6] Murty A V K, Anjanappa M and Wu Y F. "The use of magnetostrictive particle actuators for vibration attenuation of flexible beams". *Journal of Sound and Vibration*, Vol. 206, No. 2, pp 133-149, 1997.
- [7] Kumar J S, Ganesan N, Swarnamani S and Padmanabhan C., "Active control of beam with magnetostrictive layer". *Computers & Structures*, Vol.81, No.13, pp 1375-1382, 2003.
- [8] Kumar J S, Ganesan N, Swarnamani S and Padmanabhan C. "Active control of cylindrical shell with magnetostrictive layer". *Journal of Sound and Vibration*, Vol.262, No.3, pp 577-589, 2003.
- [9] Lee S J, Reddy J N and Rostam-Abadi F. "Transient analysis of laminated composite plates with embedded smart-material layers". *Finite Elements in Analysis and Design*, Vol.40, No.5-6, pp 463-483, 2004.
- [10] Pradhan S C. "Vibration suppression of FGM shells using embedded magnetostrictive layers". *International Journal of Solids and Structures*, Vol.42, No.9-10, pp 2465-2488, 2005.
- [11] Tong L and Steven G P. "Analysis and design of structural bonded joints". Dordrecht, Kluwer, 1999.
- [12] Tan P and Tong L. "Identification of delamination in a composite beam using integrated piezoelectric sensor/actuator layer". *Composite Structures*, Vol. 66, pp 391-398, 2004.
- [13] Tan P and Tong L. "A dynamic model for delamination identification using

- magnetostrictive composite patch,” *Proceedings of the 2nd International Conference on Structural Health Monitoring of Intelligent Infrastructure*, Shenzhen, China, pp 991-996, 2005.
- [14]Tan P and Tong L. “Modeling for the electro-magneto-thermo-elastic properties of piezoelectric-magnetic fiber reinforced composites”. *Composites, Part A: Applied Science and Manufacturing*, Vol. 33A, pp 631-645, 2002.
- [15]Pan E and Heyliger P R. “Free vibrations of simply supported and multilayered magneto-electro-elastic plates”. *Journal of sound and vibration*, Vol.252, No.3, pp 429-442, 2002.
- [16]Bent A A, Hagood N W and Rodgers J. “Anisotropic actuation with piezoelectric fiber composites,” *Journal of Intelligent Material Systems and Structures*, Vol. 6, pp. 338-349, 1995.
- [17]Ha S K, Keilers C and Chang F K. “Finite-element analysis of composite structures containing distributed piezoceramic sensors and actuators”. *AIAA Journal*, Vol.30, No.3, pp 772-780, 1992.
- [18]Introduction to the strand7 Finite Element Analysis System, G+D Computing Pty Ltd, Sydney, Australia, 1999.